Crystal-Structure Determination of Reduced Nicotinamide Adenine Dinucleotide Complex with Horse Liver Alcohol Dehydrogenase Maintained in Its Apo Conformation by Zinc-Bound Imidazole†

Eila Cedergren-Zeppezauer

ABSTRACT: A crystallographic study to 2.4-Å resolution of the ternary complex between horse liver alcohol dehydrogenase (LADH), NADH, and the effector molecule imidazole (Im) (LADH–NADH–Im) is presented. The ligand binding and the changes in the protein structure due to ligand interactions were interpreted from difference electron density maps calculated with phase angles derived from the refined native enzyme model. The complex crystallizes in the orthorhombic space group $C222_1$, and the enzyme structure remains in the apo conformation in which the active-site cleft is not entirely shielded from the solvent. NADH binds in an extended conformation, and the protein–coenzyme interactions are weaker compared to other complexes. The B-stereospecific side of the nicotinamide ring faces the catalytic center (LADH is known to be an A-side-specific enzyme). However, the reactive carbon atom C4 of the ring has a similar position in relation to active-center groups in this structure compared to LADH complexes where the A side of the ring faces the substrate site. The carboxamide group is situated within hydrogen-bonding distance to the sulfur of Cys-46, which is one of the three protein ligands to the active-site zinc atom. The imidazole molecule is directly ligated to the metal ion, which has a roughly tetrahedral geometry in the complex.

Horse liver alcohol dehydrogenase (LADH)[1] (EC 1.1.1.1, isoenzyme EE) catalyzes the transfer of a hydride ion from the hydroxyl-bearing carbon of an alcohol to NAD. LADH is a dimer of 40 000 daltons per subunit, and each subunit consists of two domains, the catalytic domain and the nucleotide-binding domain (Eklund et al., 1976). Figure 1 is a schematic representation of the dimer which is formed by extensive, strong contacts between the nucleotide-binding domains. The two catalytic domains are located outside this central core with the active sites in the crevices between the catalytic domains and the core. A zinc ion buried deep in each crevice is essential for catalysis. X-ray studies of two conformations of LADH with and without bound coenzyme, and with and without various additional inhibitor or substrate molecules, have shown that the crevices can be opened and closed (Eklund et al., 1981; Eklund & Brändén, 1983).

The interaction of imidazole with LADH is of particular interest, since imidazole can act either as an inhibitor or as an activator, depending upon the relative concentrations of the reactants during alcohol oxidation (Theorell & McKinley-McKee, 1961b; Collins et al., 1978). This observation has initiated numerous studies where different aspects of the structure and function of the enzyme have been examined by utilizing the properties of imidazole as effector and as metal ligand. Furthermore, the activating and inhibiting patterns of a series of heterocyclic compounds were compared, including 4(5)-substituted imidazoles, pyrazine, and triazole derivatives (Theorell et al., 1969). During these studies, the extraordinary inhibitory effect of pyrazole was discovered.

The binding of imidazole to the active-site zinc ion in the binary complex of LADH and the concomitant displacement of the metal-bound water molecule (Boiwe & Brändén, 1977; Eklund et al., 1982b) have been proven by X-ray analysis. Imidazole abolishes the pH dependencies of coenzyme binding; this finding was used as an argument in attempts to characterize the ionization behavior of the zinc-bound water molecule (Theorell & McKinley-McKee, 1961a; Taniguchi et al., 1967; Andersson et al., 1980).

Imidazole weakens nucleotide binding (Theorell & McKinley-McKee, 1961b); the multiple binding of imidazole and coenzyme fragments, fatty acids, and anions was found to exhibit a complicated inhibition pattern (Reynolds et al., 1970). Imidazole stimulates the alkylation of Cys-46 (Evans & Rabin, 1968; Reynolds & McKinley-McKee, 1969), which led to the development of alkylating agents containing an imidazole moiety as active-site-directed inhibitors (Dahl et al., 1976, 1979; Dahl & McKinley-McKee, 1977, 1981). In addition, a chromophoric substrate molecule containing the imidazole moiety 4-(2-imidazolylazo)benzaldehyde was designed for studying the transient kinetics of aldehyde reduction (Bernhard et al., 1970; Dunn, 1974; McFarland et al., 1974). A further example of a substrate with an imidazole substituent is L-histidinol. The synthesis of L-histidine can be catalyzed by LADH in a two-step reaction starting from L-histidinol with NAD as the coenzyme in both steps (Ambar, 1981; Dutler & Ambar, 1983). Although much information has been derived from the studies mentioned above, it is apparent from the relevant discussions that the complexity of the system is also increased by introducing imidazole as an effector or as part of a substrate structure. The complexity of the LADH–NADH–Im system is particularly obvious when the results from chemical relaxation measurements are interpreted (Czerlinsky et al., 1975). The authors describe the system by considering nine models of enzyme–ligand complexes which

† From the Department of Chemistry and Molecular Biology, Swedish University of Agricultural Sciences, 750 07 Uppsala, Sweden. *Received March 21, 1983; revised manuscript received July 6, 1983.* This work was supported by Grant 2767 from the Swedish Natural Science Research Council.

[1] Abbreviations: F_{obsd}, observed structure factor; F_{calcd}, calculated structure factor; Tris, tris(hydroxymethyl)aminomethane; MPD, 2-methyl-2,4-pentanediol; DACA, *trans*-4-(*N*,*N*-dimethylamino)cinnamaldehyde; H_2NADH, 1,4,5,6-tetrahydronicotinamide adenine dinucleotide; $PyAD^+$, pyridine adenine dinucleotide; io^3PyAD^+, 3-iodopyridine adenine dinucleotide; Im, imidazole; PY, pyrazole; LADH, horse liver alcohol dehydrogenase (EC 1.1.1.1); GAPDH, D-glyceraldehyde-3-phosphate dehydrogenase (EC 1.2.1.12).

0006-2960/83/0422-5761$01.50/0

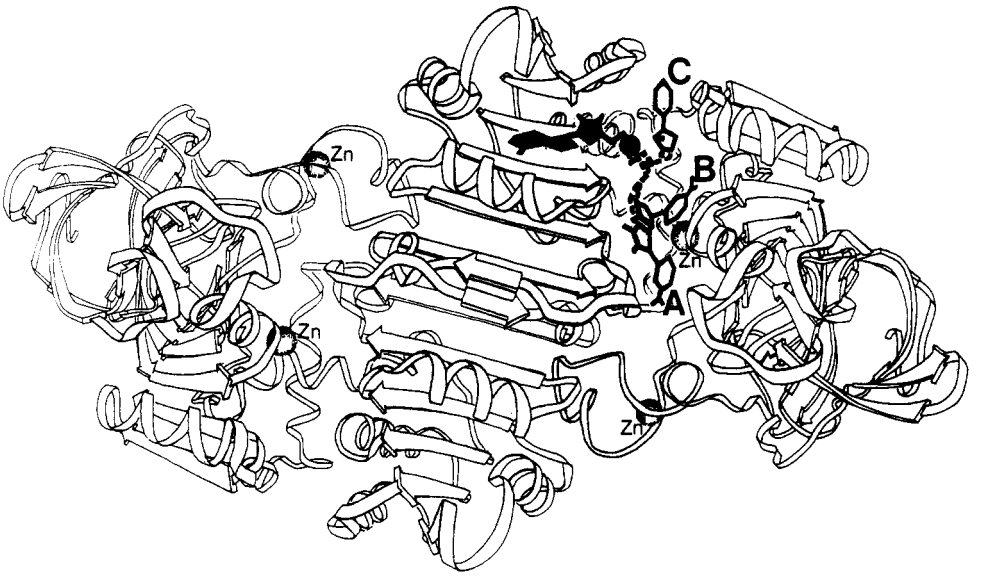

FIGURE 1: Schematic representation of the open conformation of the LADH dimer (designed by Bo Furugren). The catalytic centers are the large crevices situated between the coenzyme binding domains (central part of the molecule) and the flanking catalytic domains. Nomenclature for the secondary structure elements is described in Eklund et al. (1976). Schematic models of coenzyme molecules bound in three different conformations are shown for one subunit. The active-site zinc atom for this subunit is surrounded by models A and B. The second zinc site is not essential for catalysis. The black solid portion of the coenzyme models represents the AMP part, and the binding interactions are similar in the three cases. Label A denotes the binding site for the tetrahydronicotinamide ring in an abortive alcohol complex, label B shows the nicotinamide ring of NADH in the ternary imidazole complex, and label C is the binding site for the ring in the so-called "surface fold" of the coenzyme. See explanation under Discussion.

are interconnected. The conclusion is made that the observed relaxation time is related to the interconversion rate of two different ternary complexes between enzyme–NADH and imidazole and suggests that the imidazole ring is relocalized with reference to the nicotinamide ring during the ternary complex transition.

If LADH and NADH are cocrystallized in the presence of imidazole, orthorhombic crystals are obtained which are isomorphous to the unliganded enzyme. This is in contrast to other ternary complexes containing NADH which crystallize in triclinic or monoclinic space groups (Eklund et al., 1981). In these enzyme–NADH complexes, the protein has changed to the closed conformation. Imidazole apparently acts as an inhibitor for the coenzyme-induced transition of the open to the closed structure. This circumstance might contribute to the complex pattern found in the binding studies involving imidazole/imidazole derivatives and the coenzyme.

Detailed information of the structure of the LADH–NADH–Im complex will, hopefully, contribute to a better understanding of the mechanism of this conformational change. The present paper describes NADH and imidazole binding to the open form of the enzyme, and a comparison of coenzyme bound to the two enzyme conformations is made. In this comparison, it is emphasized that a coenzyme molecule bound to the open structure of LADH can adopt various conformations within the wide coenzyme binding cleft. Coenzyme bound to the closed structure without exception has been found in one fixed orientation. Furthermore, the comparison shows that NADH binding to LADH can differ so that either the A side (in the closed enzyme complexes) or the B side (in the LADH–NADH–Im complex) of the nicotinamide ring faces the substrate binding site.

Materials and Methods

Alcohol dehydrogenase was prepared from fresh horse liver and kindly supplied by Dr Å. Åkeson, Karolinska Institute, Stockholm. Samples of 10 mg of enzyme/mL were dialyzed at 4 °C against Tris (25 mM)–imidazole hydrochloride (5 mM), pH 7.5. NADH (0.5 mM) was added, and by slow dilution of the outer dialysate (2–3% water added), thin crystals were obtained suitable for microspectrophotometric measurements. In a final step, the crystals were dialyzed against a solution containing 5 mM Tris, 5 mM imidazole hydrochloride, pH 7.5, and 0.5 mM NADH. Crystals used for the collection of X-ray intensities were precipitated with 2-methyl-2,4-pentanediol (MPD), and crystallization was started after 1–2% (v/v) addition of the organic solvent. To avoid the appearance of microcrystals, the crystallization proceeded over a period of 5–6 weeks with a slow increase of the MPD concentration at the initial stage of crystallization. Repeated changes of the outer dialysate were made to ensure the presence of fresh NADH. Large well-ordered crystals were mounted for diffraction experiments after a few days of dialysis against a final concentration of 15% (v/v) MPD, 0.5 mM NADH, and the buffer containing 5 mM imidazole. Crystals grown in the presence or absence of solvent belong to the orthorhombic space group $C222_1$ and were examined in the microspectrophotometer.

Tris salt and NADH (grade III) were obtained from Sigma Chemical Co., St Louis, MO, and used without further purification whereas imidazole from Merck was recrystallized from heptane before use. HCl (Suprapur; Merck) and glass-distilled water were used to adjust and prepare buffer solutions. 2-Methyl-2,4-pentanediol (MPD; lot B26, Eastman Kodak Co.) was double distilled under purified nitrogen in the presence of sodium borohydride and was stored cold in the dark.

Microspectrophotometric measurements of single crystals of the LADH–NADH–Im complex were performed at Parma University, Italy, according to procedures described elsewhere (Bignetti et al., 1979).

X-ray intensities were collected at 4 °C on a Stoe four-circle diffractometer. The intensity measurements and data processing methods used have been described in detail previously (Eklund et al., 1976). The orthorhombic crystals have cell dimensions of $a = 56.0 \pm 0.1$, $b = 75.2 \pm 0.1$, and $c = 181.7$

± 0.2 Å. There is one subunit per asymmetric unit; 11 610 independent reflections were collected to 2.4-Å resolution. Twelve crystals were used, and the data set was compared with the data for the native enzyme. Scale factors and minor corrections for anisotropic disorder and radiation damages were calculated for each crystal (Eklund et al., 1981). An average R value of 13% was determined, where R is defined as $\Sigma_{hkl}||F_p| - s|F_{der}| \exp[-(u_1h^2 + u_2k^2 + u_3l^2)]|/\Sigma_{hkl}|F_p|$ for an orthorhombic case. F_p denotes structure factors for the native protein, F_{der} represents structure factors for the complex, and s is the scale factor.

Difference Fourier maps ($F_{obsd} - F_{calcd}$ or $2F_{obsd} - F_{calcd}$) were calculated by applying the phase angles obtained after crystallographic refinement of the native unliganded LADH structure. The crystallographic R factor of this enzyme model was 22% (T. A. Jones and H. Eklund, unpublished results). The model building and examination of Fourier maps were carried out on a Vector General 3404 interactive graphics display system using the FRODO program (Jones, 1978, 1982). The refined coordinates of the unliganded model were used as the starting coordinates in a model-building procedure described in detail for another orthorhombic complex of LADH (Cedergren-Zeppezauer et al., 1982). Shifts in side-chain orientations due to ligand binding were observed by examining $F_{obsd} - F_{calcd}$ Fourier maps. The model building to correct the positions was made from partial Fourier maps with coefficients $2F_{obsd} - F_{calcd}$, where the contributions of the misaligned residues were omitted in a structure factor calculation. Water positions in the active-site region were assigned from final $F_{obsd} - F_{calcd}$ maps [the structure factor calculation was based on 11 350 structure factors and 2628 atoms (including protein atoms, 1 coenzyme molecule, 1 imidazole molecule, and 2 zinc atoms) and by using an overall temperature factor]. Peak heights and the possibilities for assumed water molecules to form hydrogen bonds to neighboring atoms were the criteria used. The zinc coordinates in the complex were determined from difference Fourier maps in which the contributions from the metal atom and its ligands were omitted in a structure factor calculation. A real-space refinement procedure included in the FRODO program (T. A. Jones, unpublished results) was used. The coordinates of the zinc position in the native enzyme structure were determined by the same procedure. No crystallographic refinement of the complex has been made.

Structure factors were calculated by using the PROTEIN program by Steigemann. Stereo diagrams were plotted on a Hewlett-Packard plotter in conjunction with the VG 3404 graphics system using computer programs written by Dr. T. A. Jones. Space-filling drawings were plotted by using the PLUTO program, written by S. Motherwell and modified for proteins by E. Dodson and P. D. Evans. Coordinates for the LADH–NADH–Im structure will be deposited at the Brookhaven Protein Data Bank.

Results

Description of Ligand Binding and Comparison of the LADH–NADH–Im Complex to Other LADH Structures. (a) Conformation of the Complex. The structure of LADH in the absence of coenzyme has been determined to 2.4-Å resolution (Eklund et al., 1976). The crystals of the LADH–NADH–Im complex are isomorphous to the unliganded enzyme form; the X-ray intensities for the complex were collected to the same resolution. The conformation of this enzyme form is referred to as the apo conformation or the open conformation (Eklund & Brändén, 1983). In the present structure, NADH is bound to this open conformation. In the schematic representation of LADH (Figure 1), it is shown that the ligand-binding crevices constitute large areas of the protein molecule. The catalytic center is localized at a zinc binding site and situated deeply inside the structure. The active-site region is not entirely shielded from the surrounding medium in the LADH–NADH–Im complex since the size of the cleft which separates the domains remains constant upon NADH binding. This is in contrast to triclinic NADH complexes in which a domain rotation forms the closed conformation by narrowing the gap between the domains and thereby creating a water-free environment in the catalytic center (Eklund et al., 1981).

(b) NADH Binding. The binding of NADH in the crystalline complex was examined by microspectrophotometric measurements of single crystals. The absorption band in the 325-nm region characteristic of enzyme-bound NADH was observed (data not shown).

The difference electron density of NADH is well-defined (Figure 2), and one NADH molecule binds per subunit. Both the adenosine ribose and the nicotinamide ribose are built with a C2′ endo puckering (diagrams B and D, respectively, of Figure 2). The ADP-ribose portion of NADH is in an extended conformation, but the nicotinamide ring is oriented so that the carboxamide group interacts with the pyrophosphate bridge (Figure 3). Thus, the NADH molecule does not attain the most extended conformation possible.

The general features in the interactions between LADH and coenzyme are similar to those described previously (Eklund et al., 1981; Cedergren-Zeppezauer et al., 1982). The adenine ring is anchored to the nucleotide-binding domain, and the nicotinamide ring enters the active-site zinc region. There are, however, significant differences in the details of the coenzyme–protein interactions in this complex compared to the complexes described so far.

The side chains of Ile-224 and Ile-269 line the opening of the adenine binding pocket and constitute the hydrophobic contacts to the adenine ring (Figure 4). The side chain of Ile-224 is at a distance further than 4 Å from any ring atom. The adenine ring in general has few interactions within the distance range 3.4–4 Å with other hydrophobic residues which line the adenine pocket. The polar interaction with arginine-271 is similar to that found in other structures, and this surface side chain is localized in a well-defined density (Figure 4). Both oxygens of the adenosine ribose interact with aspartic acid-223, and lysine-228 points to the sugar moiety.

The pyrophosphate bridge does not form the tight contact to the protein which is normally observed. The distance between OP2N (Figure 3) and the nitrogen atoms at the amino end of the helix (α-B) is at the upper limit for a hydrogen-bond distance (3.3 Å). The electron density of the guanidinium group of arginine-47 is not as strong and well-defined as that found for other surface side chains fixed in definite positions due to their interaction with the coenzyme. In all coenzyme complexes examined so far, arginine-47 has been shown to bridge the cleft between the domains and to form a salt bridge with the pyrophosphate group. Such an interaction is not evident from the electron density maps of the LADH–NADH–Im complex. The weak density which is observed for residue 47 indicates an interaction with aspartic acid-50 which in turn is linked to a second arginine side chain at the surface of the catalytic domain. This Arg^{47}–Asp^{50}–Arg^{323} interaction corresponds to that observed for the triclinic complex between LADH–NADH–dimethyl sulfoxide (Eklund et al., 1981) whereas a well-defined orientation for arginine-47 has not been determined in the coenzyme-free structure (T. A. Jones, unpublished results).

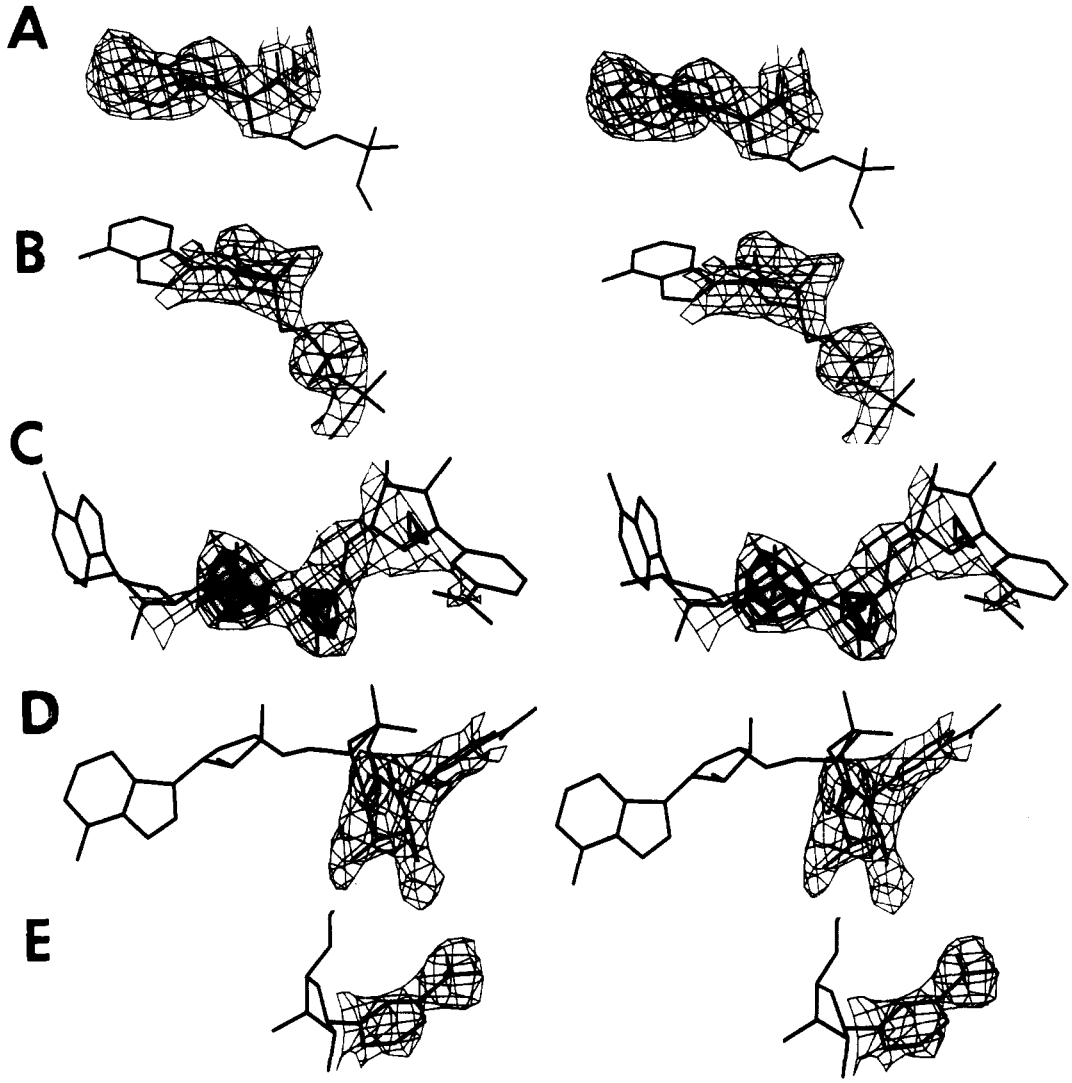

FIGURE 2: Stereo diagram showing the NADH model superimposed onto an $F_{obsd} - F_{calcd}$ Fourier map. The model is viewed from different directions in order to illustrate individual features of the density map: (A) adenine ring; (B) adenosine ribose; (C) pyrophosphate bridge with the contouring for the highest peaks in the ligand position drawn in heavy lines; (D) nicotinamide ribose; (E) nicotinamide ring.

The nicotinamide ribose is situated in the cleft between the domains with few interactions with the protein. The nearest neighbors to the O3′ oxygen are the carbonyl oxygen of residue 269 and a water molecule (Figure 4). The O2′ oxygen is at van der Waals distance to histidine-51 but does not participate in any hydrogen-bond interaction similar to that described for triclinic ternary complexes (Eklund et al., 1982a).

The localization of the nicotinamide ring is illustrated in Figure 5 and shows that the ring displaces water molecules present in the unliganded structure of LADH (T. A. Jones, unpublished results). The nicotinamide ring is that part of the coenzyme which has the tightest interactions with the protein. The side chain of valine-203 makes hydrophobic contact with the ring from one direction (Figure 4). Atoms in the active-site metal center are at van der Waals distances to the ring from the opposite direction. The electron density for the carboxamide group is clearly visible (Figure 2E), which is important in order to define the orientation of the nicotinamide ring. The carboxamide group is fixed between the guanidinium group of arginine-369, the OP1N of the pyrophosphate bridge, and the SG of cysteine-46 (Figure 3). However, the orientation of the NH_2 group or the carbonyl oxygen cannot be determined from the features of the electron density but is suggested on the basis of the nature of the neighboring protein atoms. Thus, the NH_2 group is assumed to interact with the negatively charged zinc ligand SG46 and a water molecule (Figure 3). Since the distances between the nitrogen and these two atoms are 3 Å, it would allow a hydrogen-bond interaction. This position thus seems more favorable for the NH_2 group than for the carbonyl oxygen atom. With this orientation of the carboxamide group, the oxygen atom becomes directed toward the negatively charged phosphate group, and the distance to the OP1N oxygen is 3.3 Å. The presence of the guanidinium group of arginine-369 offers the possibility for a hydrogen-bond interaction with the carbonyl oxygen. Table I summarizes the enzyme–coenzyme interactions.

The conformation of the NMN part of the coenzyme differs from that found for NADH bound to complexes in the closed conformation of LADH. Thus, the orientation of the nicotinamide ribose in relation to the coenzyme binding domain is slightly shifted, and in addition, the nicotinamide ring is rotated approximately 180°. Therefore, the ring occupies a different subsite of the active-site region in the LADH–NADH–Im complex. The B-stereospecific side of the ring is oriented toward the zinc center and the substrate binding site, which has not been observed for any LADH complex before. Another novel feature in the interactions between the coenzyme and the protein is the short distance between the carboxamide group and the zinc ligand cysteine-46.

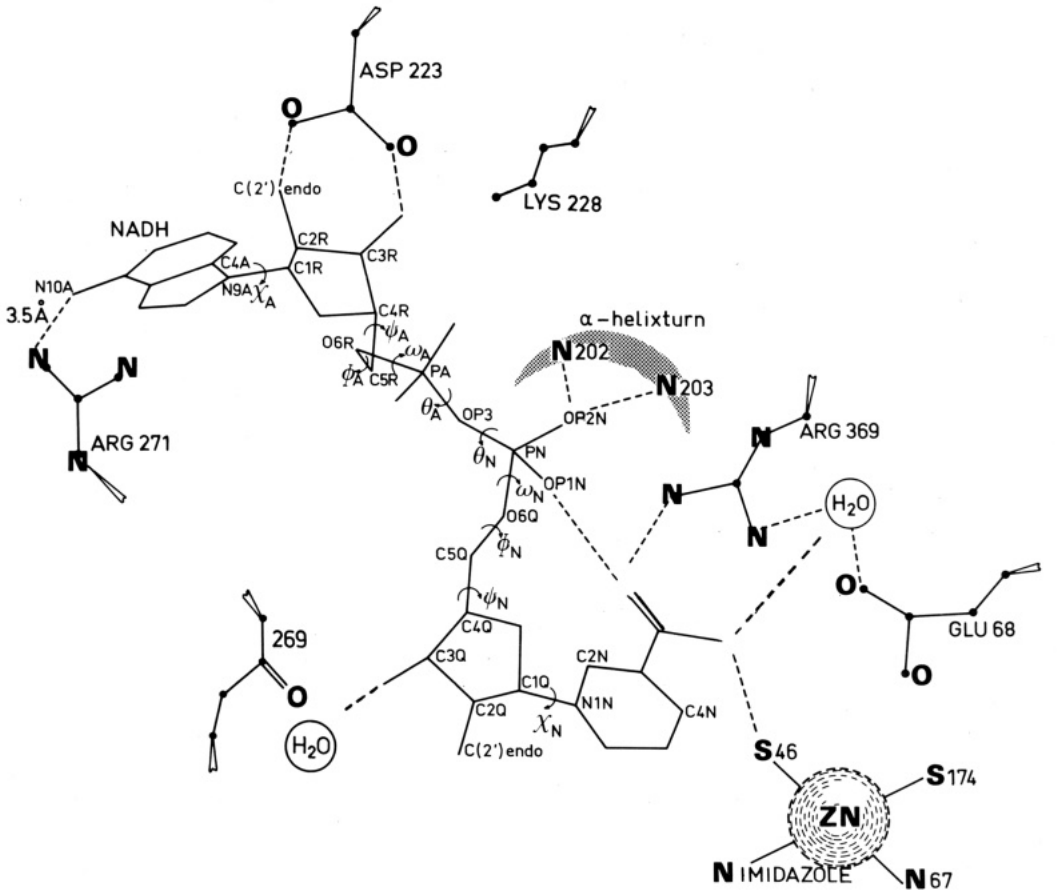

FIGURE 3: Conformation of NADH when bound in the orthorhombic structure of LADH. The dashed lines indicate distances between atoms in the distance range 2.6–3.3 Å and the interaction between arginine-271 and the adenine ring. The symbols for the torsion angles are marked, and the values are the following: $\chi_A = 163°$, $\psi_A = -37°$, $\phi_A = -175°$, $\omega_A = 40°$, $\theta_A = 142°$, $\theta_N = 152°$, $\omega_N = -69°$, $\phi_N = -179°$, $\psi_N = 164°$, $\chi_N = -54°$. The symbol convention is taken from Sundaralingam (1975).

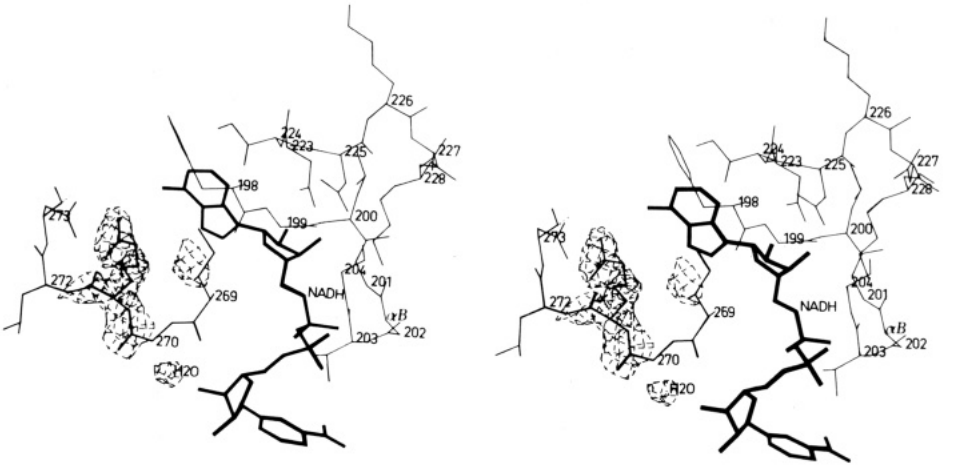

FIGURE 4: Stereo diagram of NADH bound to the open conformation of LADH. The region around arginine-271 is from an $F_{obsd} - F_{calcd}$ difference map using calculated phase angles in which the arginine side chain was omitted from the structure factor calculation. Aspartic acid-273 interacts with the guanidinium group 271. A water binding site was assigned to the peak close to the nicotinamide ribose. One helix turn in α-B is shown with the side chain of valine-203 situated above the nicotinamide ring.

Results of accessibility calculations (Lee & Richards, 1971) on the LADH–NADH–Im complex are presented in Table II. The accessible surface area is large close to the N1OA region of the adenine pocket, and the O2′ oxygen of the adenosine ribose is exposed. This is a general pattern and is observed regardless of the protein conformation in which the coenzyme molecule is bound (Cedergren-Zeppezauer et al., 1982). In the present structure, the OP1A and OP2A atoms of the pyrophosphate bridge are highly exposed whereas the second phosphate group is less accessible due to the position of the nicotinamide ring. The accessible surface area of the nicotinamide ring atoms is zero, with the exception of the C6N atom. This shows that although the cleft between the domains is open after NADH binding, the B-specific subsite for the ring is sufficiently shielded to make the C4N atom inaccessible to water. None of the water sites in the active-site region, which have been assigned from the difference density maps, is closer than 5.3 Å from the C4N atom.

Table I: Protein-Ligand Interactions in the LADH-NADH-Im Complex[a]

ligand atoms	protein atoms	residue no.	type of contact
		Adenine Ring	
C2A	CD1	Ile-269	van der Waals distances
N3A	CA	Asp-223	
	CD1	Ile-269	
C4A	CD1	Ile-269	
N7A	NE	Arg-271	
N9A	OD1	Asp-223	
N10A	NEH2	Arg-271	polar interaction 3.5 Å
		Adenosine Ribose	
C1R	CG	Asp-223	van der Waals distances
C2R	OD1	Asp-223	
O2R	OD1	Asp-223	hydrogen-bond distances
O3R	OD2	Asp-223	
O3R	NE	Lys-228	van der Waals distances
C4R	CA	Gly-199	
	OD2	Asp-223	
	CG1	Ile-269	
O5R	O	Val-268	
		Pyrophosphate Bridge	
OP1N	NEH2	Arg-369	polar interaction
OP2A	CA	Gly-201	van der Waals distances
OP2N	C	Gly-201	
	CA		
OP2N	N	Gly-202	3.2–3.4-Å distance
	N	Val-203	
		Nicotinamide Ribose	
O6Q	O	Val-268	van der Waals distances
C4Q	O	Ile-269	
C3Q	O	Ile-269	
O3Q	O	Ile-269	hydrogen-bond distance
O3Q	N	Gly-270	van der Waals distances
	N	Val-294	
O2Q	CE1	His-51	
C1Q	CA	Gly-293	
		Nicotinamide Ring	
C3N	CG2	Val-203	van der Waals distances; protein atoms
	SG	Cys-46	are 8 Å apart and interact from opposite sides of the ring
C4N	Zn		active-site Zn 4 Å
C4N	SG	Cys-46	van der Waals distances
C5N	CG2	Thr-178	
C6N	O	Val-292	
C7N	SG	Cys-46	
	CG2	Val-203	
O1N	NEH2	Arg-369	polar interaction 3.3 Å to pyrophos-
	OP1N	NADH	phate oxygen
N2N	SG	Cys-46	hydrogen-bond distances
	NEH1	Arg-369	
		Imidazole[b]	
N1	ZN	active site	metal ligand, 2.2 Å
N1	OG	Ser-48	van der Waals distances
	CZ	Phe-93	
	SG	Cys-174	
C2	CB	Ser-48	
	CE1	His-67	
	CZ	Phe-93	
N3			further than 4 Å to any protein atom
C4	OG	Ser-48	van der Waals distances
C5	SG	Cys-174	
	C4N		
	C5N		
	C6N	NADH	

[a] Only atoms of the coenzyme with neighbors within a 4-Å distance are listed. Fourteen atoms of the coenzyme molecule are further than 4 Å from any protein atom in the LADH-NADH-Im complex. For NADH bound to triclinic LADH, only four atoms are beyond the 4-Å interaction radius (H. Eklund, unpublished results). [b] Atom numbering for imidazole:

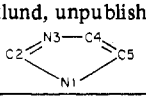

Table II: Atoms of the NADH and Imidazole Ligands Which Have an Accessible Surface Area Equal to or Greater than One Square Angstrom When Bound to the Ternary LADH Complex

atom name	accessible surface area (Å)	
N1A	5	adenine ring
N7A	8	
C8A	19	
N10A	18	
C2R	11	adenosine ribose
O2R	9	
C3R	3	
C5R	4	
PA	1	pyrophosphate bridge
OP1A	34	
OP2A	15	
OP1N	4	
C5Q	3	nicotinamide ribose
C3Q	6	
O3Q	2	
O2Q	4	
C5N	1	nicotinamide ring
C6N	5	
N3	11	imidazole ligand
C4	7	
C5	1	

Table III: Distances between the Active-Site Zinc Atom and Its Inner- and Outer-Sphere Ligands in the LADH-NADH-Imidazole Complex[a]

residue	atom name	distance from Zn (Å)	atoms within 2.7–3.2-Å distance (dots)
cysteine-46	SG	2.4	SG(46)...N2N of NADH... H_2O 3
cysteine-174	SG	2.4	
histidine-67	NE2	2.2	ND1(67)...OD1(49)
imidazole	N1	2.2	N2 of Im 3.7 Å to H_2O... OG(48)
glutamic acid-68	OE2	5.0	
H_2O 1		5.8	N(319)...H_2O 1...H_2O
H_2O 2		5.7	H_2O 2...OD1(49)...ND1(67)
H_2O 3		5.9	OE1(68)...H_2O 3...N2N of NADH...NEH1(369)

[a] Possible hydrogen-bond interactions including atoms in the vicinity of the coordination sphere are also shown.

(*c*) ***Imidazole Binding.*** The binding of imidazole in the binary enzyme complex was established previously from crystallographic data (Boiwe & Brändén, 1977; Eklund et al., 1982b). The rotation of the side chain of serine-48 is the only change reported for the binary complex. The difference electron density map for imidazole in the ternary LADH–NADH–Im structure (Figure 6) clearly shows that imidazole is ligated to zinc also in the presence of NADH. The zinc to nitrogen distance is 2.2 Å, and an outer-sphere complex via zinc-bound water is excluded.

The imidazole molecule points into the substrate binding channel, and phenylalanine-93, serine-48, and the nicotinamide ring of NADH are at van der Waals distances to the ligand. The phenyl ring is parallel to the imidazole ring whereas the nicotinamide ring is perpendiculor to it, and the orientation of the ring plane of imidazole is highly restricted by the neighborhood of the three groups. The two imidazole rings within the zinc coordination sphere, i.e, the protein ligand histidine-67 and the inhibitor, are approximately at right angles to each other (Figure 6).

Accessibility calculations (Table II) show that the C4 and N3 atoms of the imidazole ring, which point toward the direction of serine-48, are accessible. In this region, a water

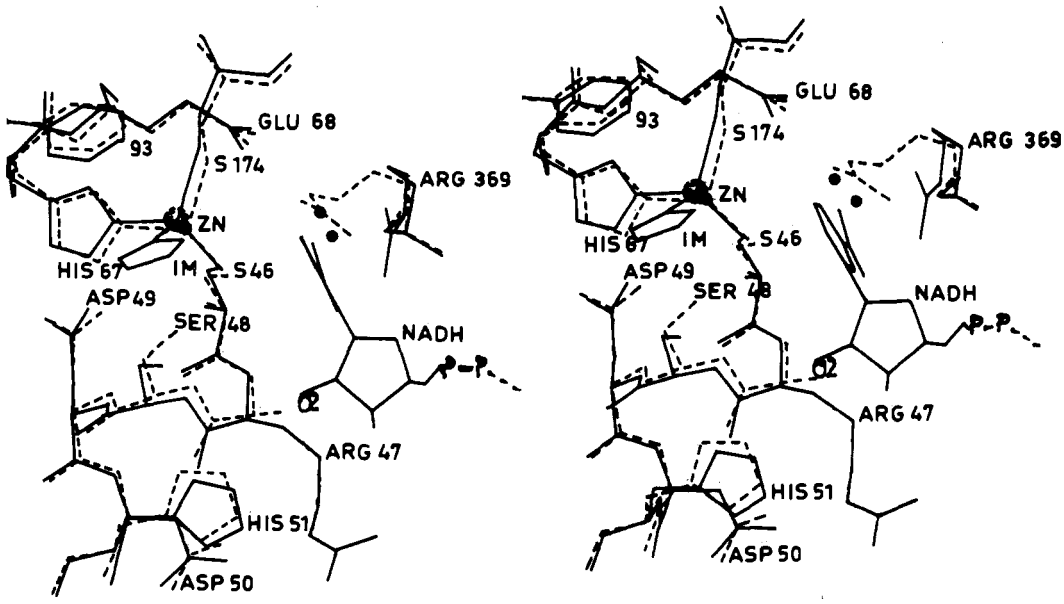

FIGURE 5: Stereo diagram comparing the native unliganded enzyme (dashed lines) and the LADH–NADH–Im complex (solid lines) at the active-site region. Im denotes the imidazole position. The two different zinc atom positions in the two structures are differentiated by the dot size at the metal center. The black dots in the nicotinamide binding site are water molecules present in the native structure (T. A. Jones, unpublished results) which are displaced in the NADH complex. At this stage of the refinement, the position of arginine-47 is not definite for the native structure.

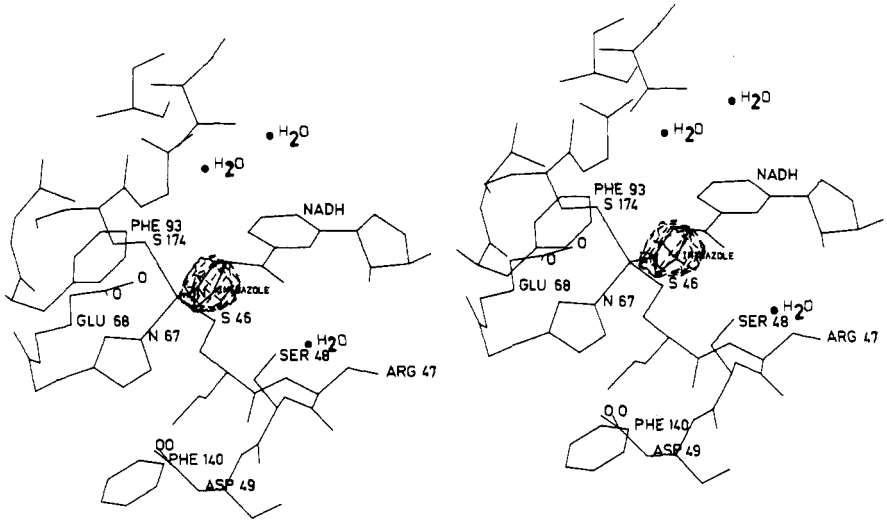

FIGURE 6: Stereo diagram showing the imidazole molecule superimposed on an $F_{obsd} - F_{calcd}$ Fourier map. The changes in the protein coordinates due to NADH binding plus the contribution from the coenzyme model have been introduced into the structure factor calculation. The water positions shown were interpreted from the same map. The structure is viewed from the interior of the catalytic domain, from the "distal" side of the zinc coordination sphere in order to visualize its relation to the buried acidic side chains 49 and 68.

binding site was assigned from the difference Fourier maps, but this water molecule is not at hydrogen-bond distance to the nitrogen atom (Table III).

No electron density which could be attributed to the precipitant molecule MPD is observed in the vicinity of the ligand. A binding site for MPD in the substrate pocket is observed in other structures of LADH (T. A. Jones, unpublished results; Cedergren-Zeppezauer et al., 1982; Schneider et al., 1983; Plapp et al., 1978), but in those complexes, the precipitant concentration is 10–15% higher than that for the crystals used in this investigation.

(d) Structural Changes in the Active-Site Region. NADH binding, with the nicotinamide ring in the B-side position (Figure 1, label B), does not induce the rotation of the catalytic domains which closes the enzyme structure. Local structural changes in the active-site area upon NADH binding are observed in the ternary imidazole complex compared to the native enzyme. The structural differences are mainly localized around the metal binding site and its nearest surroundings (Figure 5). A comparison between the zinc coordinates for the LADH–NADH–Im complex and the native enzyme shows a difference of 0.6 Å. The determinations of the zinc positions were made by real-space refinement in both structures. The shift in the zinc position is accompanied by slight reorientations of zinc ligands and neighboring amino acids and has been interpreted as a movement of the metal binding site in the direction of the substrate binding channel in the LADH–NADH–Im complex. The effect of the changed metal atom position can be illustrated by comparing imidazole binding in the binary (Boiwe & Brändén, 1977) and the ternary complexes. A displacement of bound imidazole is clearly observed in the NADH complex, and the direction of the shift is the same as for the metal atom. A schematic representation of this comparison is shown in Figure 7, which also illustrates

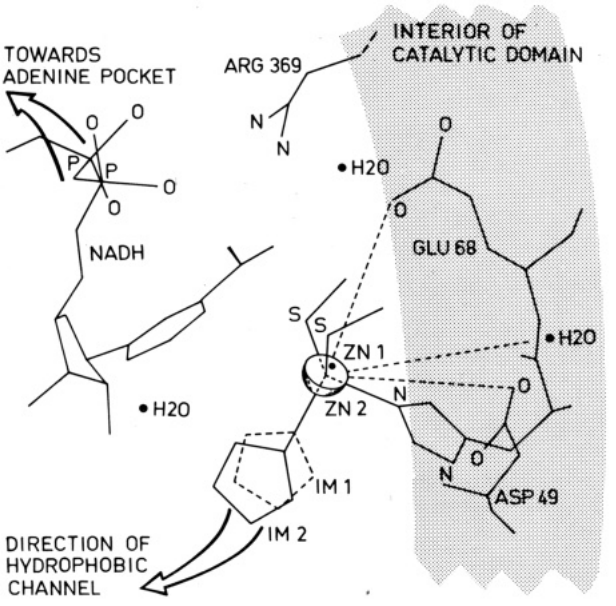

FIGURE 7: Schematic drawing showing the nearest neighbors of the active-site zinc atom in the LADH–NADH–Im complex. ZN1 (black dot) denotes the zinc position in the binary imidazole complex, and the inhibitor position, IM1 (dashed ring), is from the data of Boiwe & Brändén (1977). ZN2 (half-sphere), with the ligands SG46–SG174–N67 and ZM2, is the zinc position in the ternary complex and IM2 (solid ring) the imidazole site. The dahsed lines from one water molecule, aspartic acid-49, and glutamic acid-68 merely indicate the presence of hydrophilic groups in the interior of the protein at a distance 5–6 Å from the metal center.

the groups present within a radius of 8 Å around the zinc atom.

The zinc atom has a distorted tetrahedral geometry in this complex, similar to that observed for complexes with reduced coenzymes and zinc-bound ligands (Eklund et al., 1981, 1982a,b; Cedergren-Zeppezauer et al., 1982). The distortion from ideal tetrahedral angles is most pronounced for the SG46–Zn–SG174 angle, which is obtuse [Table II of Eklund et al. (1982b)]. In this complex, the tendency is the same (120–130°).

Compared to NADH complexes in the closed structure, an important difference is observed in the environment around the metal coordination sphere in this NADH complex. Electron densities which could not be assigned to protein or ligands are present in the vicinity of cysteine-174. These peak positions correspond to water sites in the native structure (T. A. Jones, unpublished results). This illustrates that in spite of the presence of the nicotinamide ring there is still space available at an interior region of the active site (Figure 6). Table III gives the distances between the metal atom and the ligands including three water molecules, which surround the inner coordination sphere. The carboxyl group of glutamic acid-68 is colinear with the bond direction of the imidazole ligand (Figure 7). A second carboxylate group (49) is hydrogen bonded to the zinc ligand histidine-67.

Serine-48 is rotated from its position in the apo structure away from the imidazole ligand, and the hydroxyl group interacts with a water molecule (Figure 6) situated between serine-48 and histidine-51. Neither serine-48 nor histidine-51 is engaged in coenzyme binding. Thus, the hydrogen-bonding pattern described for triclinic complexes (Eklund et al., 1982a) involving serine, histidine, and the nicotinamide ribose does not exist in the NADH–NADH–Im complex.

The side chain of arginine-369, located in the interior of the coenzyme binding cleft, moves toward the pyrophosphate bridge upon NADH binding (Figure 5), and the side-chain movement is of the order of 2–4 Å. The direct interaction between glutamatic acid-68 and arginine-369 which exists in the coenzyme-free structure is replaced by an indirect link via a water molecule (Figure 7).

Methionine-306 and leucine-309 (from the second subunit) which line the substrate channel are influenced by the ligand binding. The imidazole molecule is not large enough to establish contact with the methionine side chain, and the NADH molecule does not interact directly with these groups in the substrate channel. The methionine side chain has been rotated so that it partly blocks the entrance to the zinc sphere in this complex.

(*e*) *Comparison between Coenzyme Conformations.* Both NADH and the coenzyme analogue 1,4,5,6-tetrahydronicotinamide adenine dinucleotide (H_2NADH) in an abortive alcohol complex can bind to the open conformation of LADH. The superposition of the two models is shown in Figure 8A; the differences in conformation are most pronounced around the nicotinamide ribose. The ribose in the H_2NADH model has tight contacts to atoms in the coenzyme binding domain, and the χ_N angle, which is 45° [Table I in Cedergren-Zeppezauer et al. (1982)], gives the tetrahydronicotinamide ring an orientation in the direction of the domain–domain interface (Figure 1, label A). For NADH bound to the LADH–NADH–Im complex, this angle is −54°, and the nicotinamide ring is oriented within the active site and the ribose moiety partly overlaps the position of the tetrahydronicotinamide ring. In the open coenzyme binding cleft, there is enough space to accommodate different conformations of the coenzyme molecule. Consequently, the ring in the imidazole complex and the ring in the alcohol complex differ in their orientation and distances relative to the zinc coordination sphere.

Figure 8B displays the differences in the coenzyme conformation when the A side or the B side of the nicotinamide ring faces the active-site zinc atom. H_2NADH bound to the aldehyde complex LADH–H_2NADH–DACA (Cedergren-Zeppezauer et al., 1982) represents the A-side-specific conformation and is comparable to the binding interactions of NADH to the closed enzyme structure. The comparison thus originates from the binding of coenzyme to two different LADH structures. Nevertheless, the distance between the reactive C4N carbon in the nicotinamide ring and the metal atom is roughly 4 Å in both cases. The conformation angles for NADH in the orthorhombic complex are found in the legend of Figure 3.

Figure 9 compares the conformation of NADH in the LADH–NADH–Im complex with that of NAD bound to D-glyceraldehyde-3-phosphate dehydrogenase (GAPDH). In this comparison, the superposition of equivalent α-carbon atoms within the coenzyme binding domains (Ohlsson et al., 1974) is the basis for the transformation matrix applied to the NADH coordinates. A remarkable similarity in the orientation of the nicotinamide ring is observed. The differences in the tilt of the adenine ring originate from variations in the details of the design of the adenine binding pocket in the two enzymes.

Discussion

Coenzyme Folding. Four different conformations of the coenzyme have been observed for complexes of LADH; the dissimilarities of conformation angles are restricted to the NMN part of the coenzyme molecule. The most extended conformation is represented by the binding of coenzyme in the presence of substrates and inhibitors in the closed form of the enzyme. This binding mode corresponds to productive binding where the A side of the nicotinamide ring faces the substrate binding site. Due to the tight interactions between coenzyme and protein in this enzyme structure, extensive variations in

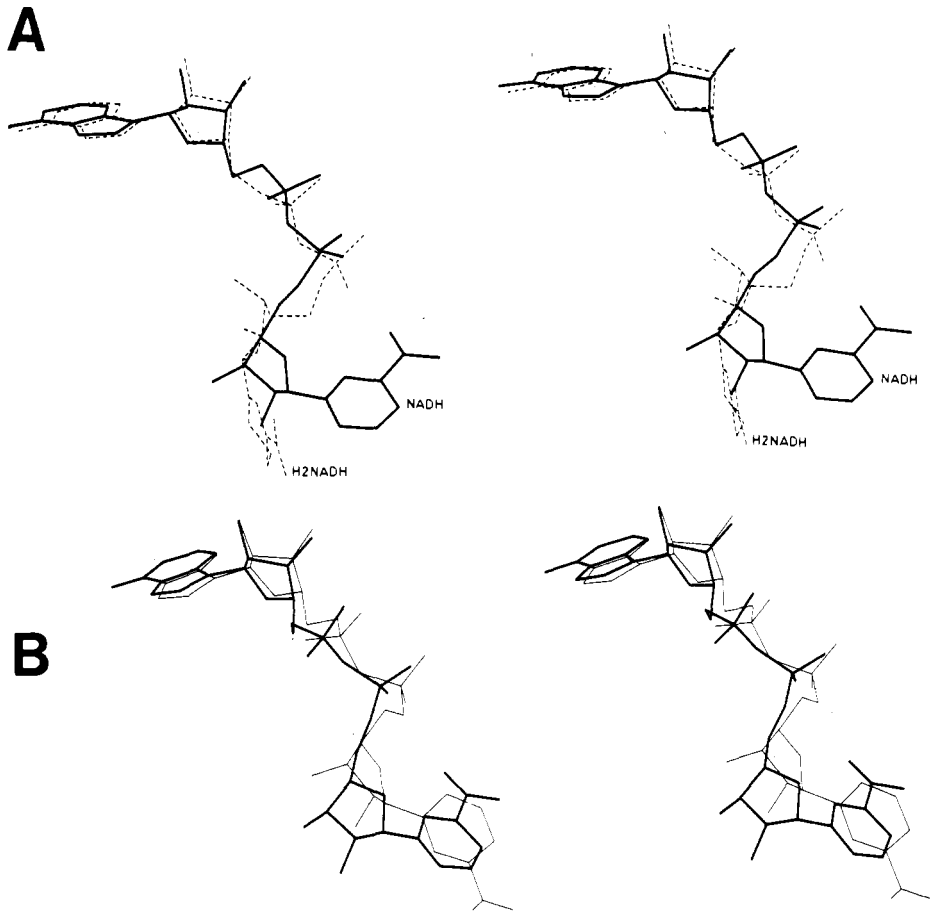

FIGURE 8: Stereo diagram comparing NADH and H_2NADH conformations when bound to LADH complexes. (A) Conformation of NADH (solid lines) in the orthorhombic LADH–NADH–Im complex and H_2NADH (dashed lines) in the orthorhombic alcohol complex LADH–H_2NADH–MPD. (B) Conformation of NADH when bound with the B side (thick lines) facing the active site in the orthorhombic structure and H_2NADH bound with the A side (thin lines) facing the active site in the triclinic structure.

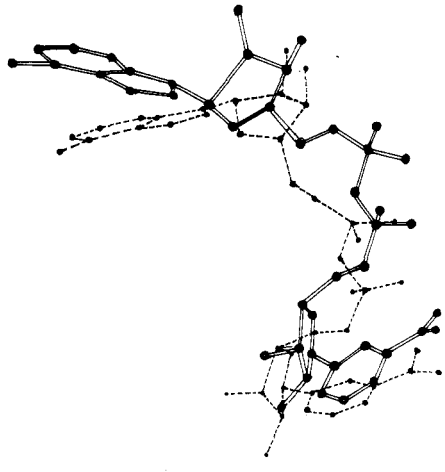

FIGURE 9: Comparison between the models of NADH bound to the ternary LADH–NADH–Im complex (open lines) and NAD bound to D-glyceraldehyde-3-phosphate dehydrogenase (dashed lines). The coordinates for the NAD molecule were obtained from the protein data bank and originate from the work of Moras et al. (1975).

the orientation of the nictonamide ring are not possible (Eklund et al., 1981).

The remaining types of coenzyme conformations observed are found for complexes in the open structure of LADH. In the presence of high concentrations of the alcohol MPD, the tetrahydronicotinamide ring of H_2NADH binds in an unproductive position and is oriented toward the interface between domains in the active-site area (Figure 1, label A). The "surface fold" of the coenzyme is a further example of unproductive binding but has been suggested to relate to the sequence of individual steps in the binding process of NAD to LADH (Samama et al., 1977, 1981). In the presence of zinc-bound imidazole, the pyridine rings of 3-iodopyridine adenine dinucleotide (io^3PyAD^+) and NAD lacking the carboxamide group ($PyAD^+$) occupy a crevice between the domains, near the adenine binding pocket (Figure 1, label C). The protein–coenzyme interactions in the io^3PyAD^+ and $PyAD^+$ complexes are further reduced compared to NADH bound in the presence of imidazole. The bulky 3-iodo substituent of io^3PyAD^+ might be unfavorable for accommodation in the vincinity of the negatively charged sulfur ligand 46 and the pyrophosphate group for steric reasons. In the case of $PyAD^+$, the possibility of positioning the nicotinamide ring through hydrogen bonds is absent. The differences in the properties between these analogues and NADH perhaps contribute to the extensive differences in binding interactions for an enzyme–imidazole complex.

A fourth type of coenzyme conformation is described in this work. The size of the active-site crevice allows a positioning of the nicotinamide ring in the proximity of the zinc center which involves a 180° rotation of the ring compared to the position in the closed structure. The consequence of this rotation is that the B side of the ring faces the substrate binding site (Figure 1, label B). It is intriguing to note the similarity in the conformation of the bound coenzyme in the LADH–NADH–Im complex and GAPDH, which shows B-side stereospecificity for hydride transfer.

It is assumed that the active form of LADH is exclusively represented by the closed structure of LADH, which is induced

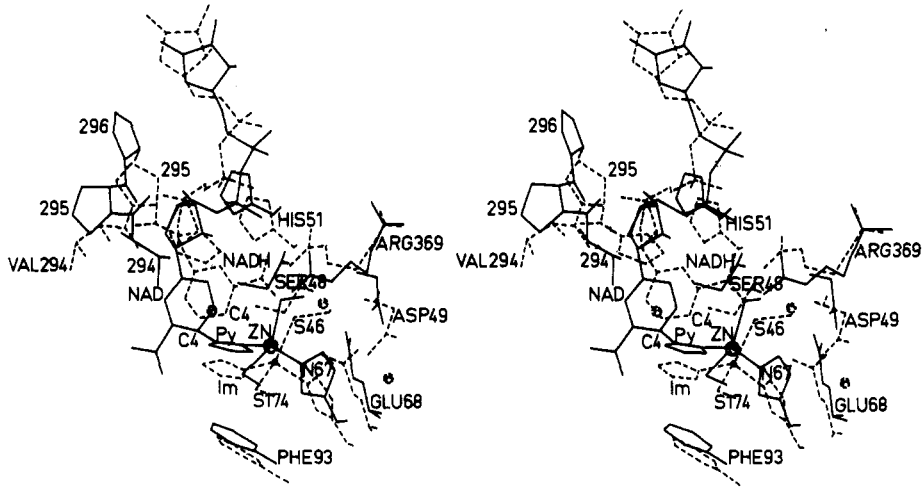

FIGURE 10: Stereo diagram comparing the active-site region of the LADH–NAD–PY complex (triclinic closed structure, full lines) with the LADH–NADH–Im complex (orthorhombic open structure, dashed lines). The differences in positions of active-site residues and the zinc center are due to the conformational change in the protein involving the rotation of the catalytic domain and the movement of the loop comprising residues 294–297. The three dots indicate water binding sites in the orthorhombic complex.

by binary complex formation with NADH. This structural transition is in accordance with the kinetic mechanism of Theorell–Chance, where the binding of coenzyme precedes substrte binding. Although this mechanism holds for alcohols, substrates have been investigated where the binding order is reversed (Ogura & Horie, 1980). It is of mechanistic interest that L-histidinol is converted to L-histidine by LADH (Ambar, 1981). A correlation between the structure of the LADH–NADH–Im complex and this particular reaction, where the substrate is an imidazole derivative, might be relevant. The binding of L-histidinol is assumed by Ambar (1981) to include the coordination of the imidazole moiety to the catalytic zinc ion at the same ligand position as the imidazole. This necessarily leads to the inhibition of the conformational change in the protein which in turn implies that the binding order will be reversed. In fact, the reversal of the binding order was suggested from mechanistic considerations for the L-histidinol to L-histidine reaction (Ambar, 1981).

Coenzyme–Protein Interactions. The concentration of imidazole used in this investigation falls within the concentration interval where imidazole acts as an activator; the rate of NADH formation is about 3 times higher when ethanol (10 mM at pH 8.65) is oxidized compared to the rate in the absence of imidazole (Ambar, 1981). NADH binding to LADH in the presence of imidazole differs substantially from NADH binding in the triclinic complexes. This is certainly the reason for the weaker binding (Theorell & McKinley-McKee, 1961a). The more facile dissociation of NADH from the LADH–NADH–Im complex is rationalized when the binding interactions are compared [Table I of this work and Table VII in Eklund et al. (1981)]. NADH is not tightly enclosed within the protein structure, since no large conformational change occurs. This has reduced the number of weak interactions and possible hydrogen bonds. Furthermore, it is not evident from the electron density maps that arginine-47 participates in coenzyme binding similar to what is observed for triclinic complexes.

The interactions between the carboxamide group and the protein seem to be related to the kind of structural changes which a coenzyme molecule is able to induce. When the carboxamide group is hydrogen bonded to atoms within the coenzyme binding domain, a rigid-body movement of the catalytic domain is induced. This conformational transition occurs irrespective of the presence or absence of a metal atom in the active site (Schneider et al., 1983). When the nicotinamide ring is rotated 180° and the carboxamide group froms hydrogen bonds with groups in the vicinity of the metal binding site, this induces local structural changes restricted to the active-site region. In the LADH–H_2NADH–MPD structure, the carboxamide group interacts with serine-48 and histidine-51, which are also located in the vicinity of the zinc binding site, but neither of these structural changes takes place (Cedergren-Zeppezauer et al., 1982).

Comparison between the Ternary Complexes with Imidazole and Pyrazole. Pyrazole (PY), an isomer of imidazole, binds to the active-site zinc atom in LADH (Eklund et al., 1982b), and in addition, an adduct with NAD can be formed. A chromophore develops with an absorption maximum slightly below that for enzyme-bound NADH. The inhibitory power of pyrazole for ethanol oxidation is high (K_i = 0.2 μM). In contrast to pyrazole, imidazole forms ternary complexes with oxidized as well as reduced coenzyme (Theorell et al., 1969). A structural comparison between the LADH–NADH–Im and the LADH–NAD–PY (Eklund et al., 1982b) complexes is now possible. The differences between a strongly inhibited enzyme and a complex at stimulating concentrations of a ligand for ethanol oxidation can thus now be described at the molecular level (Figure 10).

The nicotinamide ring in the NAD–PY adduct has the same position as that of NADH when bound in the closed enzyme structure. The bond between one of the pyrazole nitrogen atoms and the C4N carbon of NAD is formed from the A-side direction of the ring. The adjacent nitrogen atom in the pyrazole molecule is ligated to zinc (Figure 10). The ternary complex thus shows an extremely tight interaction between the protein and the ligands as well as between the ligands. A similar interaction between imidazole and coenzyme in the closed enzyme structure would bring the C4N atom within covalent bond distance to a carbon atom in the imidazole molecule. It is obvious that such a bond cannot be formed in the LADH–NADH–Im complex. The NADH binding causes an adjustment of the position of the zinc sphere and the imidazole molecule. This increases the distances between the ligand and NADH which become van der Waals distances. Figure 11 compares the two structures in a space-filling representation and illustrates the important difference in available space around the heterocyclic zinc ligands in the two cases.

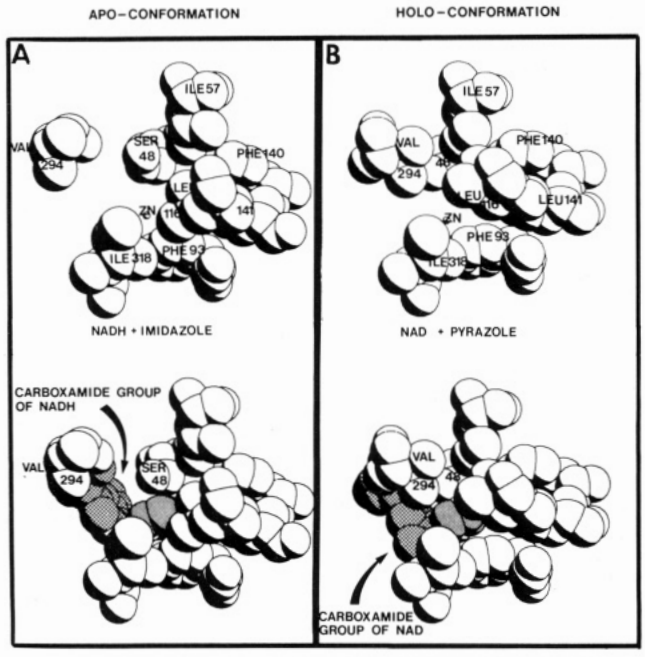

FIGURE 11: Space-filling drawing of part of the substrate channel in LADH. (Upper half) (A) Position of the zinc atom at the bottom of the binding site in the orthorhombic LADH–NADH–Im structure. For clarity, the protein ligands to zinc have been omitted, and the size of the zinc atom is diminished. (B) Same view for the triclinic LADH–NAD–PY complex (Eklund et al., 1982b). The noticeable difference between (A) and (B) is the effect of the changed orientation of valine-294. (Lower half) Same amino acids as above now with ligands added. (A) Nicotinamide ring (cross-hatched) of NADH with the orientation of the carboxamide group indicated by an arrow and the imidazole molecule (dotted) bound to the zinc atom. (B) Nicotinamide ring (cross-hatched) of NAD with the orientation of the carboxamide group in the opposite direction and the pyrazole molecule (dotted) bound to the zinc and forming the adduct with NAD on the enzyme site. The absence of a structural change upon NADH binding in complex (A) leaves the serine-48 exposed.

Acknowledgments

I am grateful to Professor R. Huber and his colleagues at the Max-Planck Institut für Biochemie (Martinsried, West Germany), who generously received me at his laboratory at an early stage of this work. I thank Dr. Alwyn Jones for access to phase angles during the course of the refinement of the LADH structure; I also thank my colleagues at the Swedish University of Agricultural Sciences, particularly Professor C.-I. Brändén and Drs. H. Eklund and B.-O. Söderberg, for continuous help and advice in computational matters. I furthermore thank Dr. E. Bignetti, who recorded the UV–visible spectra on single crystals, and I greatly appreciate discussions with Professors H. Dutler and M. Zeppezauer. Thanks are due to Anita Rogelius for help with the preparation of the manuscript and to Irmgaard Kurland for the language revision.

References

Ambar, A. (1981) Ph.D. Thesis, Nr. 6840, ETH, Zürich, Switzerland.

Andersson, P., Kvassman, J., Lindström, A., Olden, B., & Pettersson, G. (1980) *Eur. J. Biochem. 108*, 303–312.

Bernhard, S. A., Dunn, M. F., Luisi, P.-L., & Schack, P. (1970) *Biochemistry 9*, 185–192.

Bignetti, E., Rossi, G. L., & Zeppezauer, E. (1979) *FEBS Lett. 100*, 17–22.

Boiwe, T., & Brändén, C.-I. (1977) *Eur. J. Biochem. 77*, 173–179.

Cedergren-Zeppezauer, E., Samama, J.-P., & Eklund, H. (1982) *Biochemistry 21*, 4895–4908.

Collins, P. A., Hanes, C. S., & Wong, J. T.-F. (1978) *Can. J. Biochem. 56*, 1016–1020.

Czerlinsky, G. H., Wagner, M., Eriksson, J. O., & Theorell, H. (1975) *Acta Chem. Scand., Ser. B B29*, 797–810.

Dahl, K. H., & McKinley-McKee, J. S. (1977) *Eur. J. Biochem. 81*, 223–235.

Dahl, K. H., & McKinley-McKee, J. S. (1981) *J. Inorg. Biochem. 15*, 79–87.

Dahl, K. H., McKinley-McKee, J. S., & Jörnvall, H. (1976) *FEBS Lett. 71*, 287–290.

Dahl, K. H., McKinley-McKee, J. S., Beyerman, C. H., & Noorman, A. (1979) *FEBS Lett. 99*, 308–312.

Dunn, M. F. (1974) *Biochemistry 13*, 1146–1151.

Dutler, H., & Ambar, A. (1983) in *Function of Hydrolytic and Oxidative Enzymes* (Bertini, I., & Drago, R., Eds.) Reidel Publishing Co., Dordrecht, The Netherlands (in press).

Eklund, H., & Brändén, C.-I. (1983) in *Zinc Enzymes* (Spiro, T., Ed.) Wiley, New York.

Eklund, H., Nordström, B., Zeppezauer, E., Söderlund, G., Ohlsson, I., Boiwe, T., Söderberg, B.-O., Tapia, O., Brändén, C.-I., & Åkeson, Å. (1976) *J. Mol. Biol. 102*, 27–59.

Eklund, H., Samama, J. P., Wallen, L., Brändén, C.-I., Åkeson, Å., & Jones, T. A. (1981) *J. Mol. Biol. 146*, 561–587.

Eklund, H., Plapp, B. V., Samama, J.-P., & Brändén, C.-I. (1982a) *J. Biol. Chem. 257*, 14349–14358.

Eklund, H., Samama, J.-P., & Wallen, L. (1982b) *Biochemistry 21*, 4858–4866.

Evans, N., & Rabin, B. R. (1968) *Eur. J. Biochem. 4*, 548–554.

Jones, T. A. (1978) *J. Appl. Crystallogr. 11*, 268–272.

Jones, T. A. (1982) in *Computational Crystallography* (Sayre, D., Ed.) pp 303–317, Oxford University Press, New York.

Lee, B., & Richards, F. M. (1971) *J. Mol. Biol. 55*, 379–400.

McFarland, J. T., Chu, Y. H., & Jacobs, J. W. (1974) *Biochemistry 13*, 65–69.

Moras, D., Olsen, K. W., Sabesan, M. N., Buehner, M., Ford, G. C., & Rossman, M. G. (1975) *J. Biol. Chem. 250*, 9137–9162.

Ogura, Y., & Horie, S. (1980) *J. Biochem. (Tokyo) 88*, 1135–1139.

Ohlsson, I., Nordström, B., & Brändén, C.-I. (1974) *J. Mol. Biol. 89*, 339–354.

Plapp, B. V., Eklund, H., & Brändén, C.-I. (1978) *J. Mol. Biol. 122*, 23–32.

Reynolds, C. H., & McKinley-McKee, J. S. (1969) *Eur. J. Biochem. 10*, 474–478.

Reynolds, C. H., Morris, D. L., & McKinley-McKee, J. S. (1970) *Eur. J. Biochem. 14*, 14–26.

Samama, J.-P., Zeppezauer, E., Biellmann, J.-F., & Brändén, C.-I. (1977) *Eur. J. Biochem. 81*, 403–409.

Samama, J.-P., Wrixon, A. D., & Biellmann, J.-F. (1981) *Eur. J. Biochem. 118*, 479–486.

Schneider, G., Eklund, H., Cedergren-Zeppezauer, E., & Zeppezauer, M. (1983) *EMBO J. 2*, 685–689.

Sundaralingam, M. (1975) *Structure and Conformation of Nucleic Acids and Proteins-Nucleic Acid Interactions* (Sundaralingam, M., & Raou, S. T., Eds.) p 488, University Park Press, Baltimore, MD.

Taniguchi, S., Theorell, H., & Åkeson, Å. (1967) *Acta Chem. Scand. 21*, 1903–1920.
Theorell, H., & McKinley-McKee, J. S. (1961a) *Acta Chem. Scand. 15*, 1811–1833.
Theorell, H., & McKinley-McKee, J. S. (1961b) *Acta Chem. Scand. 15*, 1834–1865.
Theorell, H., Yonetani, T., & Sjöberg, B. (1969) *Acta Chem. Scand. 23*, 255–260.

Crystal Structure of a Sweet Protein, Monellin, at 5.5-Å Resolution†

Gail Tomlinson,‡ Craig Ogata, Whan-chul Shin,§ and Sung-Hou Kim*

ABSTRACT: A 5.5-Å resolution crystal structure of an intensely sweet protein, monellin, has been determined on the basis of four isomorphous heavy-atom derivatives. The structure reveals many protruded features unlike most globular proteins. There are four monellin molecules in the asymmetric unit of the crystal and two dimer molecules related by a noncrystallographic twofold axis.

Monellin, isolated from *Dioscoreophyllum cumensii*, a tropic berry also called the serendipity berry, is a protein which tastes extremely sweet (van der Wel, 1972; Morris & Cagan, 1972). The sweet sensation elicited by monellin is roughly 100 000 times as intense as that of sucrose when compared on a molar basis and 3000 times as intense when compared on a milligram basis. Monellin has excellent potential for being used as a natural substitute sweetener.

The only other protein known to taste sweet is thaumatin, which is also derived from an African berry. Although monellin and thaumatin display little sequence homology (Frank & Zuber, 1976; Iyengar et al., 1978), immunological studies show cross-reactivity (van der Wel & Bel, 1978; Hough & Edwardson, 1978), suggesting that the two sweet proteins may indeed share common structural features which may be involved in the sweet taste phenomenon. Furthermore, one of these studies (Hough & Edwardson, 1978) shows that several other sweet compounds, such as saccharin, L-aspartyl-L-phenylalanyl methyl ester, sucrose derivatives, cyclamates, and neohesperidin dihydrochalcone, compete for the antibody raised against thaumatin. This suggests that these compounds may have structural features common, in parts, with thaumatin.

Monellin is a small protein with a molecular weight of 10 700. It contains no carbohydrate. The molecule is composed of two nonidentical peptide chains (Bohak & Li, 1976), and the tertiary structure of the molecule is essential for the taste effect to take place as demonstrated by circular dichroism studies using a variety of denaturing conditions (Jirgensons, 1976).

Large well-shaped crystals were obtained from a solution containing 4 mg/mL monellin (purchased from Worthington Biochemical Corp., Freehold, NJ), 15% (w/w) polyethylene glycol (average molecular weight of 6000), and 10 mM phosphate buffer at pH 7.2 and equilibrated with 33.3% (w/w) polyethylene glycol at 4 °C by a vapor diffusion method (Tomlinson & Kim, 1981). Monellin crystallizes in a space group $P2_1$ with cell parameters of 39.1 × 71.5 × 86.9 Å^3 with $\beta = 107.6°$. The density of the crystals (1.88/cm^3) was determined by using a density gradient formed by xylene and carbon tetrachloride and calibrated with a series of CsCl solutions. Partial specific volume of monellin calculated from the amino acid composition is 0.73 cm^3/g. Molecular weight of an asymmetric unit of the unit cell calculated by using the above values is 46 000, corresponding to about four monellin molecules consisting of eight peptides. This gives V_m, the ratio of the volume per unit molecular weight, to be 2.7 Å^3/dalton, which is normal for protein crystals. Still photographs show that the crystals diffract better than 2.3-Å resolution.

Experimental Procedures

X-ray diffraction data have been collected for four heavy-atom derivatives by using an ω scan mode on a four-circle automatic diffractometer at 4 °C. The heavy-atom compounds used were $KAuCl_4$, K_2PtCl_4, $HgCl_2$, and $Pd(NH_3)_2Cl_2$. Buffered solution of each compound was introduced into monellin crystals in mother liquor at a concentration of 0.5–1.0 mM and left for 1–60 days before data collection.

Phase refinement for the protein data was carried out by the method of multiple isomorphous replacement (Blow & Crick, 1959; Dickerson et al., 1961). During the first five cycles of the least-squares refinement, occupancies were held constant while positional parameters and temperature factors were varied. During the next five cycles, temperature factors were held constant and the positional parameters and occupancies were varied. The final positions, number of sites, R modulus

$$\Sigma||F_{PH} - |F_P + f_H||/\Sigma f_H$$

and weighted R modulus are listed in Table I.

In calculating the electron density map at 5.5-Å resolution, in order to minimize any rippling effect due to termination of Fourier series at 5.5 Å, an artificial temperature factor of 300 Å^2 was applied. With this temperature factor the structure factor amplitudes at 5.5-Å resolution are reduced to about 9% of its original value, thus effectively eliminating any series termination errors. This approach significantly improved the background noise level of the electron density map without noticeably altering electron density within the molecular envelope, thus facilitating identification of the molecular boundary.

To search for possible local rotation axes using a method developed by Rossmann and Blow (Rossmann & Blow, 1962), and facilitated by Crowther (Crowther, 1971), rotation search

† From the Department of Chemistry, University of California, Berkeley, California 94720. *Received April 13, 1983.* Supported in part by National Institutes of Health Grant NS15174 and by a grant from the U.S. Department of Energy.
‡ Present address: George Washington University, School of Medicine and Health Science, Washington, DC.
§ Present address: Department of Chemistry, Seoul National University, Seoul, Korea.

0006-2960/83/0422-5772$01.50/0